A three-dimensional model for analyzing the effects of salmon redds on hyporheic exchange and egg pocket habitat

Daniele Tonina and John M. Buffington

Abstract: A three-dimensional fluid dynamics model is developed to capture the spatial complexity of the effects of salmon redds on channel hydraulics, hyporheic exchange, and egg pocket habitat. We use the model to partition the relative influences of redd topography versus altered hydraulic conductivity (winnowing of fines during spawning) on egg pocket conditions for a simulated pool–riffle channel with a redd placed at the pool tail. Predictions show that altered hydraulic conductivity is the primary factor for enhancing hyporheic velocities and dissolved oxygen content within the egg pocket. Furthermore, the simulations indicate that redds induce hyporheic circulation that is nested within that caused by pool–riffle topography and that spawning-related changes in hyporheic velocities and dissolved oxygen content could create conditions suitable for incubation in locations that otherwise would be unfavorable (reinforcing the notion that salmonids actively modify their environment in ways that may be beneficial to their progeny).

Résumé : Nous mettons au point un modèle tridimensionnel de dynamique des fluides afin de capturer la complexité spatiale des effets des frayères à saumons sur l'hydraulique du chenal, les échanges hyporhéiques et l'habitat des poches d'œufs. Le modèle nous sert à départager l'influence relative de la topographie des frayères par rapport à celle de la conductivité hydraulique altérée (la séparation des particules fines durant la fraie) sur les conditions des poches d'œufs dans un canal expérimental simulant une alternance de zones profonde et rapide et possédant une frayère placée à l'aval de la zone profonde. Les prédictions montrent que le changement de conductivité hydraulique est le facteur principal qui augmente les vitesses hyporhéiques et le contenu en oxygène dissous au sein de la poche des œufs. De plus, les simulations indiquent que les frayères produisent une circulation hyporhéique qui est emboîtée dans celle causée par la topographie des zones profonde et rapide; les changements reliés à la fraie dans la vitesse hyporhéique et le contenu en oxygène dissous pourraient créer des conditions adéquates pour l'incubation dans des sites qui seraient par ailleurs inadéquats (ce qui renforce la notion que les salmonidés modifient activement leur environnement selon des modes qui peuvent être bénéfiques à leurs rejetons).

[Traduit par la Rédaction]

Introduction

It has long been recognized that a critical component of the salmonid life cycle is successful spawning and incubation of offspring (Chapman 1988). Salmonids bury their eggs in riverbed gravels within the hyporheic zone, which is the saturated band of sediment that surrounds alluvial rivers and across which biophysical gradients develop through porous sediment (Hendricks and White 1991; Edwards 1998). During spawning, a female salmonid uses her tail to direct and accelerate river water toward the streambed by turning on her side and undulating her body, excavating a depression in which she lays her eggs (Fig. 1) (Burner 1951; Chapman 1988; Groot and Margolis 1991). She then digs another pit in front of the first and covers the eggs that have been fertilized by one or more males, after which she may lay another clutch of eggs in the new pit and repeat the process several more times. The resultant egg nest (or redd) has a characteristic pit and tailspill topography (Fig. 1*c*) and may contain one or more egg pockets. The depth of the egg pocket depends on many factors, size of the fish, size of the sediment, depth of the water, depth of alluvium, and velocity of flow, but is on the order of tens of centimetres and scales with the size of the fish (DeVries 1997). After hatching, the alevins live within the shallow hyporheic zone for some time before emerging into the stream (Groot and Margolis 1991; Quinn 2005).

Redd construction alters local physical characteristics of the streambed that may have important implications for the success of buried salmonid embryos. It creates macroscale bed topography that alters channel hydraulics and streambed pressure. These changes are believed to generate local hyporheic circulation that pumps surface water through the redd

Received 13 November 2008. Accepted 29 July 2009. Published on the NRC Research Press Web site at cjfas.nrc.ca on 19 November 2009.
J20878

Paper handled by Associate Editor Michael Bradford.

D. Tonina.[1] University of Idaho Center for Ecohydraulics Research, 322 East Front Street, Suite 340, Boise, ID 83702, USA.
J.M. Buffington. US Forest Service, Rocky Mountain Research Station, 322 East Front Street, Suite 401, Boise, ID 83702, USA.

[1]Corresponding author (e-mail: dtonina@uidaho.edu).

Fig. 1. Longitudinal view of (*a*) a pool–riffle bedform with hyporheic exchange induced by bed topography (light blue lines), (*b*) construction of a salmon redd at the pool tail, and (*c*) the post-spawning channel and redd topography showing the increased hydraulic conductivity within the redd due to winnowing of fine material during spawning ($K_{redd} > > K_{aq}$, where K_{aq} is the hydraulic conductivity of the undisturbed bed material) and the hypothesized redd-induced hyporheic exchange (dark blue lines) nested within the bedform-induced exchange. Modified from Burner (1951).

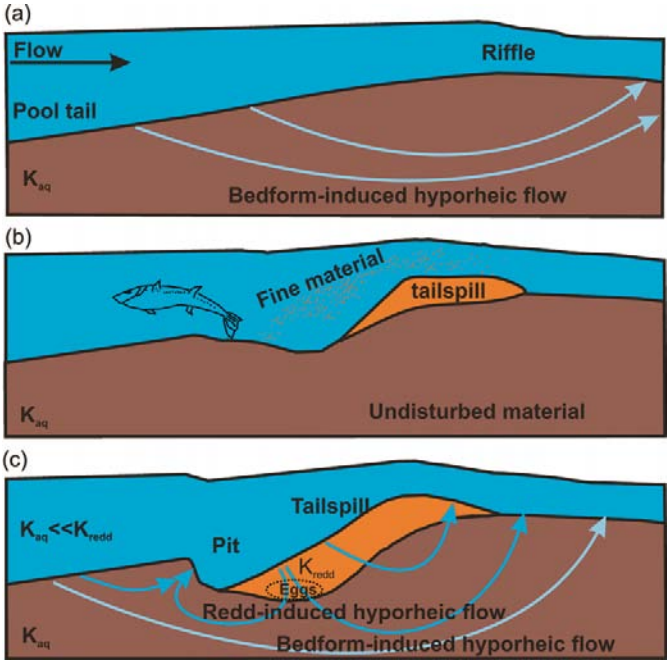

(e.g., Cooper 1965; Kondolf 2000; Zimmermann and Lapointe 2005*a*) (Fig. 1*c*) similar to that observed for fluvial dunes (Thibodeaux and Boyle 1987). This redd-induced flux is biologically important, as it is believed to oxygenate buried salmonid embryos, remove waste products, and enhance embryo survival to emergence (Coble 1961; Alonso et al. 1988; Greig et al. 2007). During redd construction, the female also winnows fine material out of the nest, leaving relatively coarse, porous sediment with higher hydraulic conductivity (less resistance to subsurface flow) than the surrounding sediment (Everest et al. 1987; Chapman 1988; Montgomery et al. 1996). This likely enhances the rate of hyporheic exchange through the redd, potentially decreasing egg mortality rates (McNeil and Ahnell 1964; Lapointe et al. 2004; Zimmermann and Lapointe 2005*b*). Hence, salmonids modify their environment in ways that may be beneficial to the success of their offspring (White 1990; Montgomery et al. 1996).

Although it is widely believed that redd topography induces local hyporheic exchange, to our knowledge, only one study has demonstrated it (Carling et al. 2006). Numerous investigators claim that redds generate hyporheic exchange, but inspection of the underlying data reveals that these claims are based on analogy with the effects of two-dimensional dune-like topography (e.g., Cooper 1965; Vaux 1962; White 1990) or are based on observations of hyporheic exchange through pool–riffle topography (Stuart 1953, 1956; Kondolf 2000), not actual studies of redds. While it is expected that redd topography will induce local hyporheic circulation, studies examining the structure and magnitude of the exchange as well as its relationship to exchange caused by surrounding fluvial bedforms are lacking. In particular, Edwards (1998) suggested that redd-scale exchange is overwhelmed by the larger-scale exchange of fluvial bedforms, with the implication being that redd-induced hyporheic exchange may be physically and biologically insignificant. However, this hypothesis has not been explored. The structure, magnitude, and significance of redd-induced hyporheic exchange likely depend on the specific three-dimensional shape of the redd and its location within the channel in relation to surrounding bedforms and associated hydraulics.

In this study, we develop a three-dimensional fluid dynamics model to examine predicted patterns and magnitudes of redd-induced hyporheic exchange and to assess the ecological significance for incubating eggs. Unlike previous numerical studies of hyporheic exchange through redds (Alonso et al. 1988), we explicitly account for the effects of redd topography on channel hydraulics and streambed pressures that drive hyporheic circulation. Additionally, we test whether bedform-induced hyporheic flow supersedes redd-induced exchange (Edwards 1998). Furthermore, while spawning is known to alter channel topography and hydraulic conductivity of the streambed, the relative effects of these factors on hyporheic exchange and dissolved oxygen (DO) content within egg pockets have not been well studied. Prior studies have examined one or the other of these factors (Alonso et al. 1988; Carling et al. 2006) or have examined their combined effects (Zimmermann and Lapointe 2005*a*). Here, we partition these factors to quantify their relative influence. Finally, we examine whether the depth of alluvium affects hyporheic exchange and consequent egg pocket habitat.

To address the above issues, numerical simulations were conducted for a gravel, pool–riffle channel with and without a redd placed at the pool tail, a typical location for spawning that capitalizes on downwelling hyporheic flux forced by channel topography (Stuart 1953; Bjornn and Reiser 1991; Kondolf 2000). We use a three-dimensional model because pool–riffle channels have complex hydraulics and strongly three-dimensional hyporheic exchange that is not well predicted by two-dimensional approaches (Tonina and Buffington 2007).

Materials and methods

Overview

The analysis presented in this paper capitalizes on recent advances in computational fluid dynamics (CFD) with improved capabilities for modeling in-stream flow over complex topography (Hodskinson 1996; Nicholas and Sambrook Smith 1999; Ma et al. 2002) and its relationship to hyporheic exchange (Tonina and Buffington 2007). In this study, a finite element CFD package (Fluent 6.1; Fluent Inc., Lebanon, New Hampshire) was coupled with a three-dimensional pumping model (Tonina and Buffington 2007) to predict hyporheic exchange. The spatial distribution of streambed pressure was predicted as a function of channel hydraulics as modified by bed topography and used to drive a Darcy model for subsurface (hyporheic) flow (Tonina and

Buffington 2007). Modeling hyporheic flow, rather than measuring it in the field, has the advantage of being a nonintrusive approach capable of resolving the flow field in detail. The analysis provides a three-dimensional examination of how redds are predicted to modify both in-stream and hyporheic flow and the degree to which these changes are predicted to enhance the velocity and DO content through an egg pocket.

Channel characteristics

Field data from Whiting et al. (1999) were used to simulate a typical headwater gravel-bed river used by spawning Chinook salmon (*Oncorhynchus tshawytscha*) in central Idaho. A pool–riffle morphology was selected, characterized by a sequence of alternate bars in a straight reach (Fig. 2). We chose a bankfull channel width (w_B) of 6 m as a lower limit of channel size suitable for Chinook spawning, comparable with that observed in the study area (D. Isaak, US Forest Service, 322 East Front Street, Suite 401, Boise, ID 83702, USA, unpublished data). Hydraulic geometry relationships developed by Whiting et al. (1999) were used to predict the bankfull discharge (Q_B) and depth (h_B) corresponding to this 6 m wide channel.

Pool–riffle morphology is commonly characterized in terms of the frequency and amplitude of pool and riffle bed forms (e.g., Carling and Orr 2000). Because self-formed pool–riffle channels typically have a mean pool spacing (λ) of five to seven bankfull widths (Leopold et al. 1964; Keller and Melhorn 1978), we selected a pool wavelength of six bankfull widths for our analysis. Bedform amplitude (Δ) is defined here by the residual pool depth, which is the difference in elevation between the riffle crest and the pool bottom (Lisle and Hilton 1992). We used a ratio of bedform amplitude to wavelength (Δ/λ) equal to 0.01, which is typical of self-formed pool–riffle channels in western North America (Prestegaard 1983; Buffington and Montgomery 1999). The geometric characteristics of the simulated reach are summarized in Table 1.

The bed material in our analysis is assumed to be a gravel–sand mixture typical of pool–riffle channels with a median diameter of 60 mm and with a prespawning hydraulic conductivity of 1.5×10^{-4} m·s^{-1}, similar to that measured in gravel patches selected by spawning salmonids (Malcolm et al. 2004; Geist 2005). The simulations were conducted for a half-bankfull flow for which the bed is assumed to be immobile other than local sediment motion caused by spawning. This assumption is reasonable given that gravel-bed rivers typically have a near-bankfull threshold for significant bed mobility (Leopold et al. 1964; Parker 1978; Andrews 1984).

Redd topography and location

The redd dimensions used in our analysis are based on a combination of field measurements made in tributaries of the Middle Fork Salmon River, central Idaho, and values reported in the literature for Chinook salmon (Alonso et al. 1988; King and Thurow 2000) (Fig. 3).

Salmonids tend to spawn in hydraulic transitional zones that generate hyporheic exchange (Burner 1951; Stuart 1956; Vronskiy 1972), such as pool–riffle transitions (Fig. 1*a*) where there is strong interaction between the channel topography and flow, but they may also spawn in any available gravel patch when high densities of spawning occur (Schuett-Hames 1996). At pool–riffle transitions, salmon and trout typically spawn in the pool tail where downwelling hyporheic fluxes occur (Bjornn and Reiser 1991; Baxter and Hauer 2000; Kondolf 2000) (Fig. 1), but they may also spawn at riffle crests (Chapman 1943; Vronskiy 1972) and downstream of the riffle crest in upwelling zones (Geist and Dauble 1998; Hanrahan 2007). Furthermore, they generally orient their redds parallel to the current (R. Thurow, US Forest Service, Rocky Mountain Research Station, 322 East Front Street, Suite 401, Boise, Idaho 83702, USA, personal communication). In our simulations, the redd is inserted along the centerline of the stream at the pool tail with its tailspill ending at the riffle crest and its longitudinal axis oriented with the flow, which meanders around the exposed bars during the time of spawning (Fig. 2).

Numerical model

Scaling

The reach used in the numerical simulation was a 1:6.6 scale model of a natural channel (referred to as the prototype), where the geometric length scale, L_L, is 6.6 m (Table 1). Although numerical models do not require scaling, we selected this approach to compare the model with laboratory flume studies (Tonina and Buffington 2007). Dynamic similitude between the model and prototype requires the matching of both Reynolds and Froude numbers, which is not typically possible (Chadwick and Morfett 1997), forcing the selection of one or the other and the potential for imperfect similitude (i.e., introduction of errors in the scaling of channel hydraulics). However, errors caused by Froude number scaling are negligible at large Reynolds numbers (fully turbulent flow, as was the case for our analysis). Therefore, we chose Froude number scaling between the prototype and model ($Fr_p = Fr_m$, where the Froude number is $Fr = u/\sqrt{gh}$, u, h, and g are the mean flow velocity, depth, and gravitational acceleration, respectively, and the subscripts "m" and "p" denote the model and the prototype, respectively). All of the geometric dimensions of the channel are scaled by L_L:

$$(1) \qquad \frac{(w_B)_p}{(w_B)_m} = \frac{(h_B)_p}{(h_B)_m} = \frac{(\Delta)_p}{(\Delta)_m} = \frac{(\lambda)_p}{(\lambda)_m} = L_L$$

The redd prototype was also scaled by the geometric factor L_L when inserted into the numerical model. The undistorted Froude number model ($Fr_p = Fr_m$) requires that the velocity for the prototype and model are scaled as

$$(2) \qquad \frac{u_p}{u_m} = \sqrt{L_L}$$

Surface hydraulics

The simulations were carried out with Fluent 6.1 (Fluent Inc., Lebanon, New Hampshire), a CFD package that solves the Reynolds equations for unsteady and incompressible flow. The Realizable κ–ε model (Shih et al. 1995) was chosen for the turbulence closure because it performs well in simulating three-dimensional flows with large rates of strain and boundary curvature (Fluent Inc. 2003). We treated

Fig. 2. Simulated pool–riffle topography used in this study. The red ellipse, the black line passing through the ellipse, and the red dots on this line indicate the redd location, the longitudinal transect through the redd, and the locations of simulated subsurface velocity profiles (P1, P2, and P3) (Fig. 3), respectively. Brown shading indicates exposed topography and blue-green shading is submerged topography.

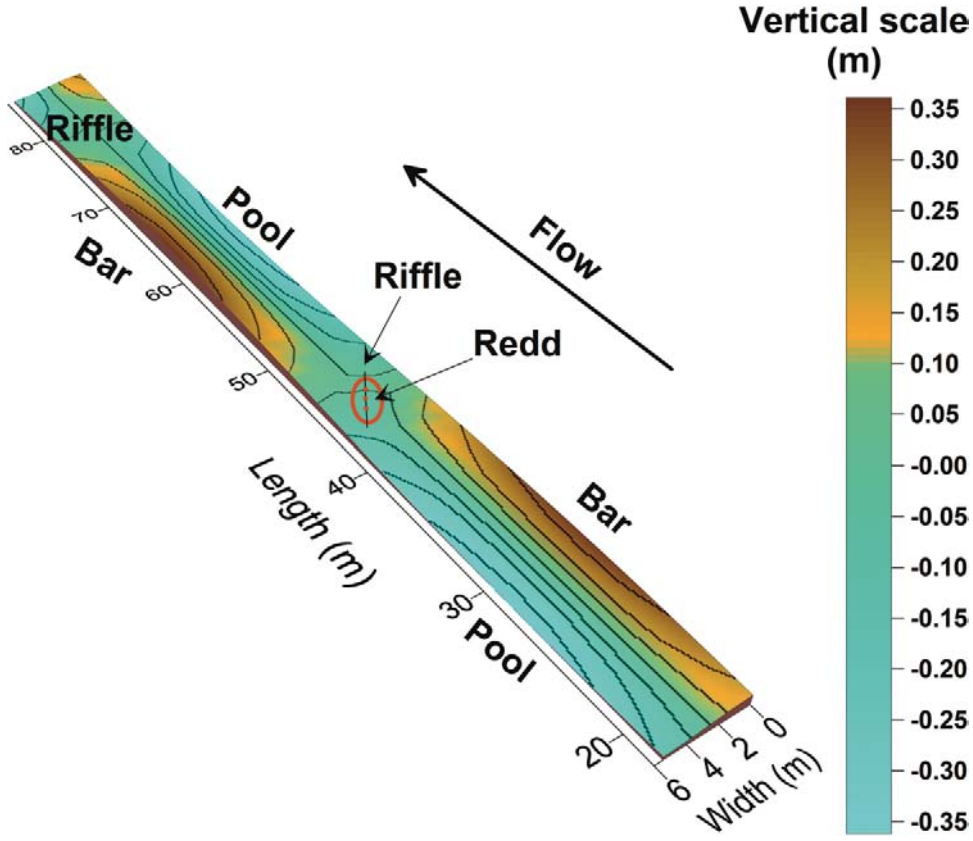

Table 1. Channel characteristics.

Channel characteristics	Field values (Whiting et al. 1999)	Prototype	Numerical model
w_B (m)	6.37	6	0.91
h_B (m)	0.32	0.35	0.053
Q_B ($m^3 \cdot s^{-1}$)	2	2	0.018
Δ (m)		0.35	0.053
λ (m)		36	5.46

Note: $w_B$is the bankfull width, h_B is the bankfull depth, Q_B is the bankfull discharge, and Δ and λ are, respectively, the amplitude and wavelength of the pool–riffle topography.

the near-wall flow with the standard wall function (Fluent Inc. 2003). To simulate an open-channel flow, we used the volume of fluid option that models a two-phase system: water and air (Hirt and Nichols 1981). The presence of air enabled the software to determine the water surface topography by simultaneously solving water and air flow fields. This method gives a more accurate representation of the flow field than the commonly used fixed-lid approach in which the water surface is specified a priori (e.g., Nicholas and Sambrook Smith 1999).

During the CFD simulations, the riverbed was treated as an immobile and impermeable wall decoupled from the hyporheic system. Although riverbeds are in fact permeable, with mass and momentum transfer occurring across the surface–subsurface boundary (Ruff and Gelhar 1972; Vollmer et al. 2002; Packman et al. 2004), this exchange is typically small (e.g., Packman and Bencala 1999) (i.e., hyporheic flux does not strongly affect the surface flow).

Hyporheic exchange

After the CFD package determined the surface flow field and streambed pressure distribution, the bed surface was modeled as a pressure inlet (permeable surface) for coupling the surface and subsurface domains and predicting hyporheic exchange as a Darcy flow (Darcy 1856; Freeze and Cherry 1979). A three-dimensional pumping model (Tonina and Buffington 2007) was used to predict the Darcy flow field and consequent hyporheic exchange as a function of spatial variations in streambed pressure, implemented in Fluent. The first pool-to-pool sequence was chosen as the study section and was meshed with hexahedral elements with 3 cm sides (Tonina and Buffington 2007). Seven boundary conditions characterize this domain: the two river sides, bottom, and exposed parts of the bars (all modeled as impervious layers (no-flow boundary)), the bed surface (set as a pressure inlet boundary), and the upstream and downstream ends (modeled as periodic boundaries). Periodic boundaries ensure

Fig. 3. Redd topography showing (*a*) locations of subsurface (hyporheic) velocity profiles discussed in the paper (P1 within the redd pit, P2 within the middle of the tailspill, and P3 within the tailspill crest) and (*b*) dimensions along the longitudinal axis of the redd (a = 0.5 m, b = 0.2 m, c = 2.2 m, d = 1.0 m, e = 0.2 m, and f = 0.1 m) with redd width 2.1 m and pit width 0.8 m.

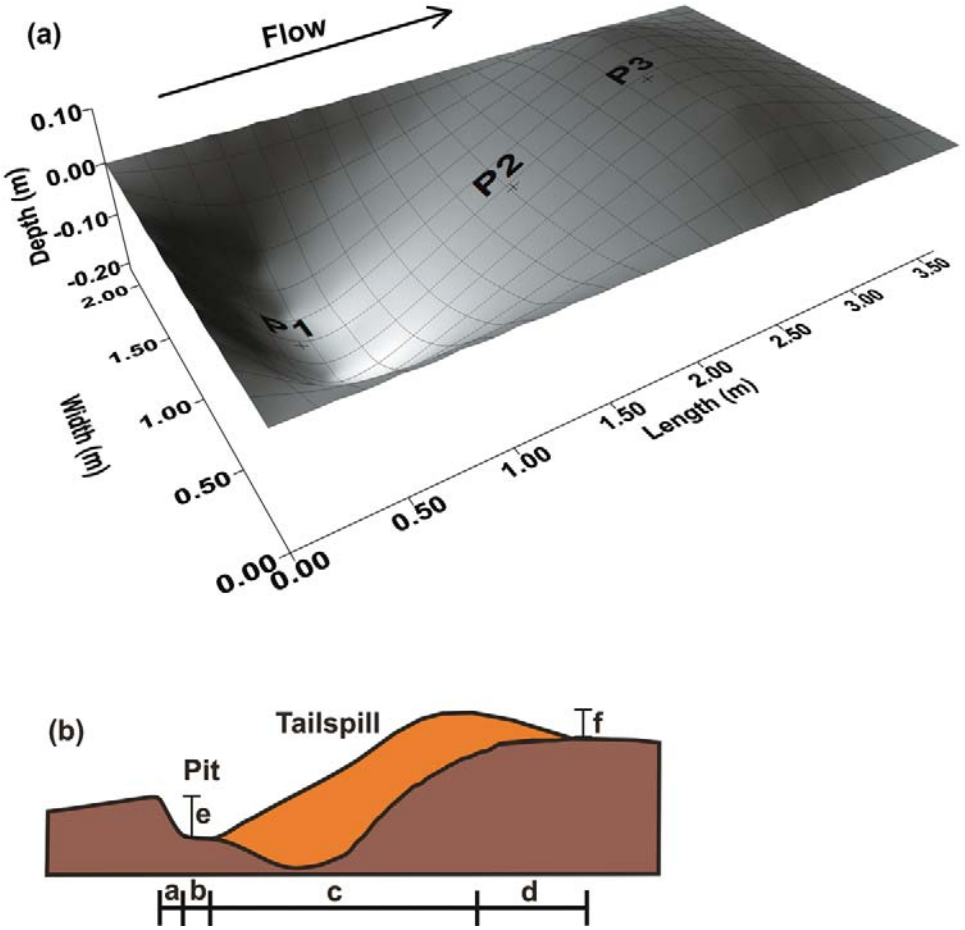

that what is going out from one boundary is going into the other one, forming an infinite reach of pool–riffle sequences.

Once the hyporheic flow field was solved using Darcy's law (Tonina and Buffington 2007, section 2), the particle tracking method was applied to evaluate flow paths and residence times for particles numerically injected into the bed at different locations (Tonina and Buffington 2007). This method traces hyporheic trajectories and predicts travel times for surface flow to pass through the subsurface sediment before reentering the river, excluding flow paths that are lost to the deep aquifer and that do not reemerge into the river within the model domain. Upwelling and downwelling areas are determined by the direction of the hyporheic fluxes normal to the sediment surface; fluxes exiting and entering the sediment at the streambed interface indicate upwelling and downwelling areas, respectively. To further assess the potential effects of the redd, hyporheic velocity profiles were predicted at three locations along the longitudinal profile of the redd (Fig. 3, P1, P2, and P3) and at the same coordinates for the case without the redd.

Dissolved oxygen concentration

DO concentration is a critical factor for the growth and development of salmonid embryos incubating within eggs buried in the streambed as well as for later growth stages when alevins dwell among the gravel interstices before emerging into the stream (Chapman 1988).

To investigate the DO profile within the sediment, we modeled oxygen concentration as a function of hyporheic advection, molecular diffusion, D_m, and biological consumption. DO is brought into the sediment by downwelling fluxes of river water and is used by microinvertebrates, biofilms, and other animals that dwell in the sediment interstices (Findlay and Sobczak 1999). The oxygen uptake by these organisms is referred to as sediment oxygen demand (SOD). SOD depends on oxygen concentration and varies with depth as well as organic and inorganic transformations, but because of the uncertainty of the magnitude of this variable, we assumed a constant value equal to 2.64 $g \cdot m^{-3} \cdot day^{-1}$ (Huang et al. 2001) throughout the sediment domain. To scale the hyporheic model of SOD, we matched the Reynolds numbers in the model and prototype, resulting in a scaled SOD of 0.38 $g \cdot m^{-3} \cdot day^{-1}$ (Tonina 2005). The D_m value for oxygen in water was estimated from the Wilke and Chang (1955) formula

$$D_m = 7.4 \times 10^{-8} \frac{T\sqrt{\psi M}}{\mu V} \quad (3)$$

where T is the absolute temperature of the water in degrees

Kelvin (288.15 K), ψ is a parameter for the solvent capacity of the water, 2.26, M is the molecular weight of the water, 18 g·mol^{-1}, μ is the water viscosity in centipoises, and V is the molar volume of oxygen, 25.6 cm^3·g^{-1}.

The DO transport equation used in the model is

$$\frac{\partial \mathrm{DO}}{\partial t} + \boldsymbol{v}\nabla \mathrm{DO} = D_\mathrm{m}\nabla^2 \mathrm{DO} - \mathrm{SOD} \quad (4)$$

where t is time and $\boldsymbol{v}$ is the local velocity vector within a given cell of the subsurface numerical domain. Equation 4 indicates that the change in DO with time is a function of the velocity field (second term on the left side), molecular diffusion (first term on the right side), and oxygen uptake within the sediment (second term on the right side). The DO value is a function of temperature; in cold water, DO has a higher saturation value. We assumed boundary conditions of 10 mg DO·L^{-1} at the bed surface (a typical value of DO in well-oxygenated rivers at 15 °C (Wetzel 1983)) and 2 mg DO·L^{-1} at the bottom of the alluvium (an arbitrary low concentration), with a critical deprivation limit of 5–6 mg·L^{-1} (Bjornn and Reiser 1991; Greig et al. 2005). We applied eq. 4 to assess the importance of redds on the DO distribution within the sediment.

Experiments

We investigated four scenarios: (1) a gravel pool–riffle morphology with deep alluvium (depth = 0.5λ, where λ is the bedform wavelength), (2) the same morphology with shallow alluvium (depth = 0.05λ), (3) case 1 with a redd superimposed at the tail of the pool, and (4) case 2 with a redd also superimposed at the tail of the pool. The first two scenarios focus on prespawning conditions (hyporheic exchange driven by channel topography, as mediated by alluvial depth; Tonina 2005). The second two scenarios add the effects of redd topography on channel hydraulics, streambed pressure, and consequent hyporheic exchange. To partition the effects of redd topography versus altered hydraulic conductivity due to winnowing of fine sediment during spawning, the second two scenarios were further subdivided into two cases: (*a*) constant hydraulic conductivity within the streambed (fictitious case of no winnowing that isolates the effects of redd topography only) versus (*b*) higher hydraulic conductivity in the redd than the surrounding sediment (combined effects of redd topography and winnowing). The hydraulic conductivity of the undisturbed streambed material was set equal to 1.5×10^{-4} m·s^{-1} (scaled to $K_{aq} = 10^{-3}$ m·s^{-1}), a value that is found in gravel-bed rivers bearing redds (Malcolm et al. 2004; Geist 2005). The redd hydraulic conductivity was set to 7.57×10^{-3} m·s^{-1} (scaled to $K_{redd} = 0.05$ m·s^{-1}), which is comparable with values observed in redds (Gustafson-Greenwood and Moring 1991).

Finally, an estimate of the vertical extent of the egg pocket is needed, as hyporheic flow characteristics vary with depth and position in the subsurface environment. The vertical location of the egg pocket depends on the depth at which the females lay their eggs. DeVries (1997) reported that average depths for the top and bottom of Chinook salmon egg pockets are approximately 15 and 50 cm below the original bed surface, respectively. Consequently, we assumed these values as upper and lower limits of the egg pocket. A constant discharge of 1 m^3·s^{-1} corresponding to half-bankfull discharge was used to simulate a medium flow.

Results

River hydraulics

Prior to spawning, the simulations predict that at medium discharge, parts of the bars are dry and the flow meanders around them, accelerating over the riffle and diving into the pool (Fig. 4*a*). The high-velocity core (Dietrich and Smith 1983) swings from the left to the right side of the channel, remaining in the outer side of the pool. Downstream of the riffle crest on the inner side of the pool, a large eddy is predicted that creates a dead zone where the water moves slowly. The model also predicts that the water surface elevation rises as it approaches the riffle and then declines downstream (Fig. 5*a*). Channel hydraulics similar to the above predictions were observed in flume experiments conducted for the same bed topography but at a slightly higher discharge (Tonina and Buffington 2007).

After spawning, the predicted spatial distribution of velocity is locally modified by the presence of the redd (Fig. 4*b*). The current accelerates as it approaches the riffle, but the redd pit causes flow separation and turbulence that retards the acceleration and the velocity suddenly drops. The flow separation at the upstream edge of the pit creates a recirculating vortex characterized by low pressure, similar to what happens on the lee side of a dune (Raudkivi 1963; Middleton and Southard 1984; McLean and Smith 1986). The water then accelerates again as the flow is forced to shallow over the tailspill of the redd, but the location of the high-velocity core remains essentially unchanged. The presence of the pit and the tailspill additionally affect the predicted water surface elevation, which falls at the beginning of the pit, rises again, and eventually lowers over the tailspill (Fig. 5*b*).

Similar to the changes in velocity, the predicted pressure distribution over the riverbed is locally altered by the redd (Fig. 6). Prior to spawning, the model predicts that high-pressure areas are located in the outer part of the upstream pool tail, while lower-pressure areas occur in the inner part of the pool downstream of the riffle.

As expected, the redd locally modifies these patterns, creating a high-pressure area before the tailspill and a low-pressure zone both within the pit and downstream of the tailspill. As discussed above, the low-pressure zone in the pit stems from the flow separation at the upstream lip of the pit. A complementary high-pressure zone occurs just downstream of the pit where the boundary layer reattaches as the flow climbs the tailspill (Fig. 6*b*).

Hyporheic exchange

Prior to spawning, hyporheic exchange is controlled by bed topography, with downwelling areas predicted to occur on the upstream side of the riffle (high-pressure zone) and upwelling areas predicted to occur downstream of the riffle crest and in the recirculation zone close to the bar (both low-pressure zones, as discussed above) (Fig. 7*a*).

After spawning, predicted reach-scale patterns of hyporheic exchange are similar but are locally altered by the redd, which imposes upwelling in areas where downwelling would have otherwise occurred and imposes downwelling in

Fig. 4. Predicted water-surface velocities in the study reach (*a*) without and (*b*) with redd topography. Contour lines represent bed topography with a contour interval of 0.005 m. All dimensions are model-scaled.

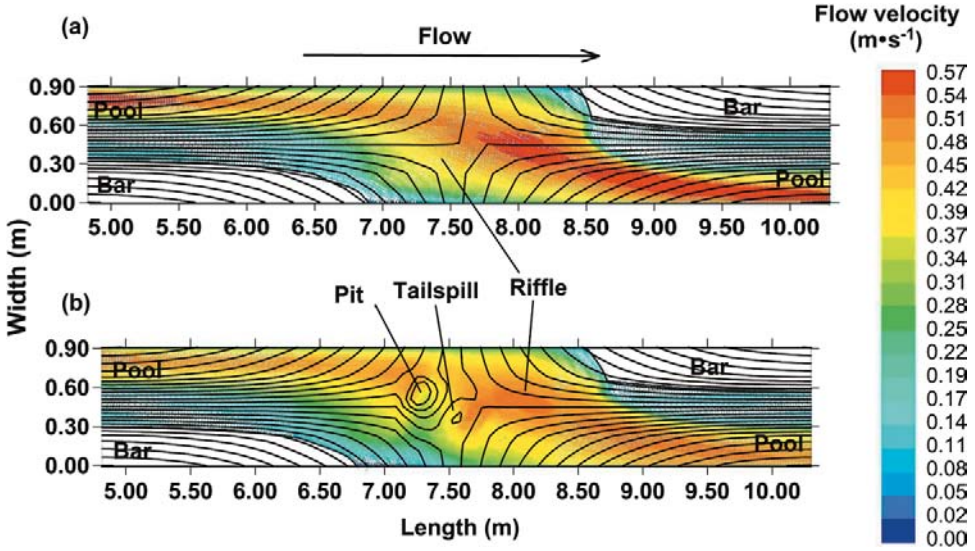

Fig. 5. Predicted water surface topography in the study reach (*a*) without and (*b*) with a redd superimposed at the pool tail. All dimensions are model-scaled.

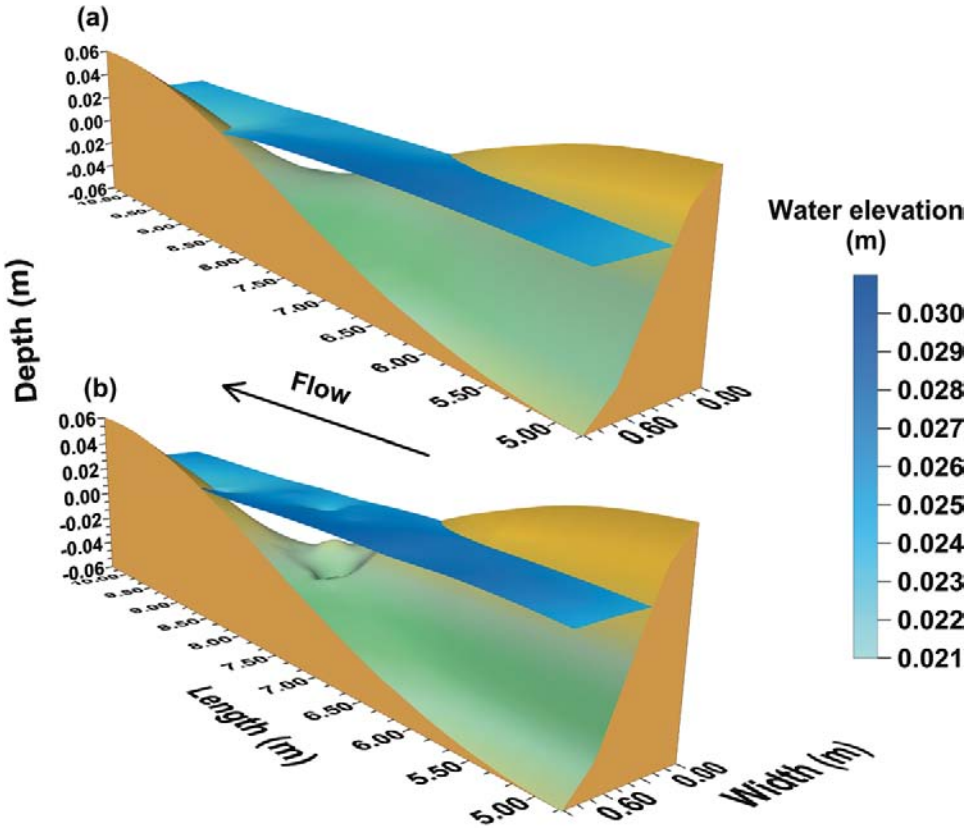

locations where upwelling would have occurred (cf. Figs. 7*a* and 7*b*). Recirculating eddies in the redd pit and downstream of the tailspill crest create low-pressure zones (Fig. 6*b*) that force upwelling downstream of the tailspill and in the upstream half of the redd pit (Figs. 7*b* and 8). In contrast, the high-pressure zone over the tailspill (Fig. 6*b*) forces downwelling through the tailspill, where the eggs are located (Figs. 7*b* and 8).

The simulations also predict that the redd receives instream water laterally because of the presence of the bar and the three-dimensionality of the channel topography and hydraulics. As flow exits the pool and is topographically forced over the riffle, the water surface rises approaching the bar head (Fig. 5), thereby intensifying the pressure over the sediment (Fig. 6*b*). This high-pressure zone drives river water and downwelling flux toward the redd. These effects

Fig. 6. Predicted streambed pressure distribution in the study reach (*a*) without and (*b*) with redd topography. Contour lines represent bed topography with a contour interval of 0.005 m. All dimensions are model-scaled.

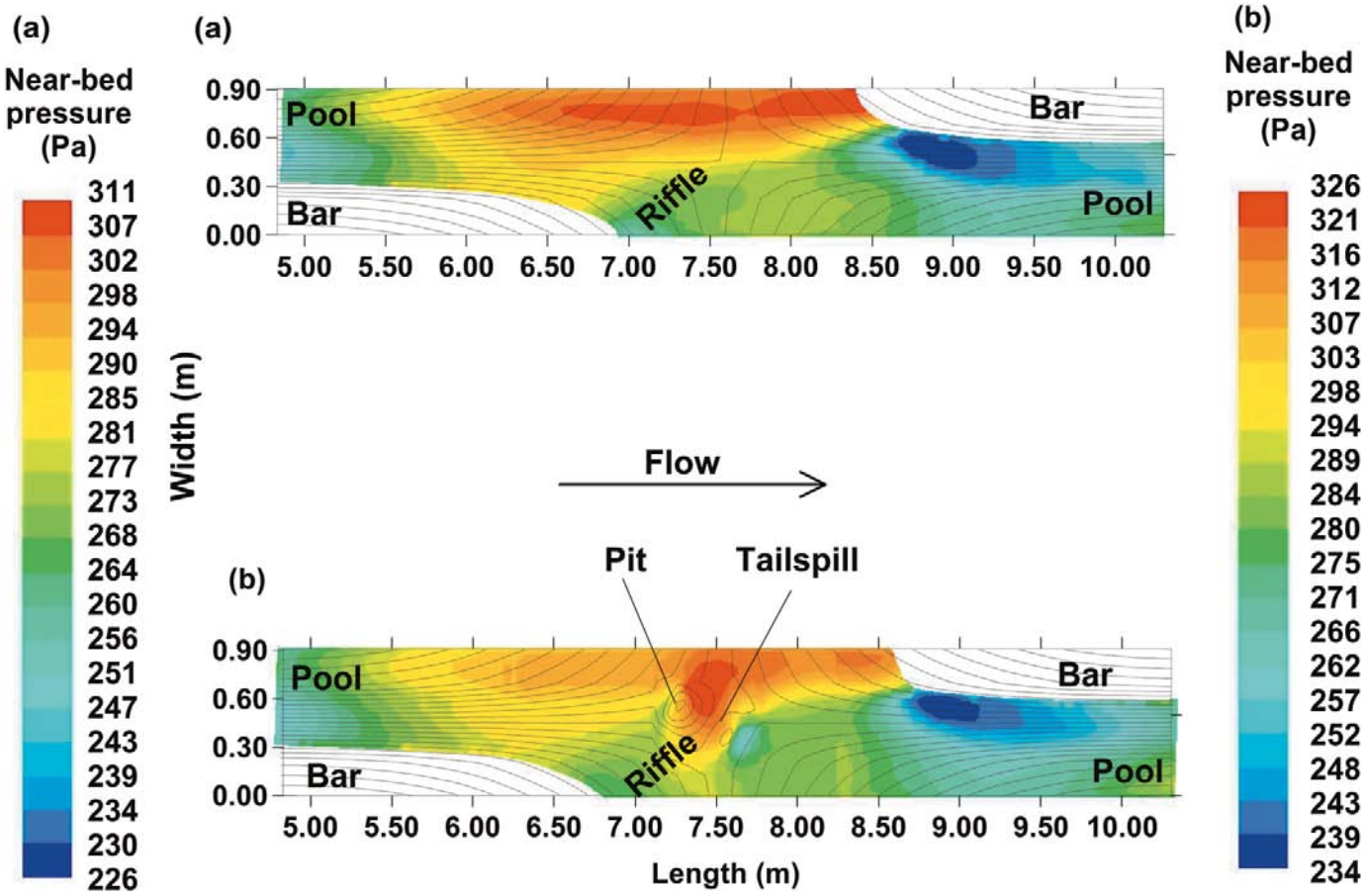

of lateral flow are not captured by previous two-dimensional models (Alonso et al. 1988).

The predicted longitudinal pattern of hyporheic circulation caused by the redd (Fig. 8) is similar to that observed in laboratory studies of two-dimensional bedforms (Cooper 1965) and for a redd placed on a planar bed (Carling et al. 2006). However, our simulations reveal that the redd-induced hyporheic exchange is superimposed on the bedform-induced hyporheic flow (Fig. 8). The redd generates its own near-surface hyporheic cells that are nested within the larger hyporheic circulation caused by the pool–riffle topography of the channel and is not overridden by the larger circulation, as suggested by Edwards (1998).

Depth of alluvium and hyporheic flow paths

The depth of alluvium does not affect the location and spatial pattern of upwelling and downwelling areas (Fig. 9 insets), which, instead, are functions of the streambed pressure distribution as influenced by bed topography and channel hydraulics (e.g., Tóth 1963; Tonina and Buffington 2009). However, the depth of alluvium does affect path lengths of hyporheic flow and consequent rates of hyporheic exchange (Fig. 9). Furthermore, with deep alluvium, predicted hyporheic pathlines are three-dimensional close to the surface, while deeper pathlines show a more two-dimensional behavior (Fig. 9*a*). In contrast, when the depth of alluvium is shallow, the predicted hyporheic flow is strongly three-dimensional and interacts with (is limited by) the impervious layer (i.e., clay, bedrock) (Fig. 9*b*). The flow paths penetrate down into the sediment until they reach the impervious layer and then they travel parallel to the bottom to emerge at a low-pressure zone on the streambed.

Hyporheic velocity and residence time distribution

Our predictions indicate that redd topography alone causes a three- to fourfold increase in velocity within the egg pocket (Fig. 10, P2 and P3) compared with that induced by the larger-scale pool–riffle topography. In contrast, the combined effects of redd topography and altered hydraulic conductivity (winnowing of fines) cause the velocity to increase by two orders of magnitude (Fig. 10, P2 and P3), a substantially greater effect than redd topography alone. We also find that the depth of alluvium does not significantly change predicted velocities within the redd (cf. Figs. 10*a* and 10*b*). However, for shallow alluvium, the velocities for a given location are slightly lower than for the case of deep alluvium.

The predicted flux of in-stream water that is present within the sediment at different residence times, and therefore available for biochemical reaction in the hyporheic environment, is shown in Fig. 11. Predictions indicate that the redd topography alone has little effect on the reach-average downwelling flux and residence time, but the change in hydraulic conductivity due to spawning has a substantial impact, in-

Fig. 7. Predicted upwelling (dark shading) and downwelling (light shading) areas in the study reach with shallow alluvium (0.05λ) (*a*) without and (*b*) with redd topography. Contour lines represent bed topography with a contour interval of 0.005 m. All dimensions are model-scaled.

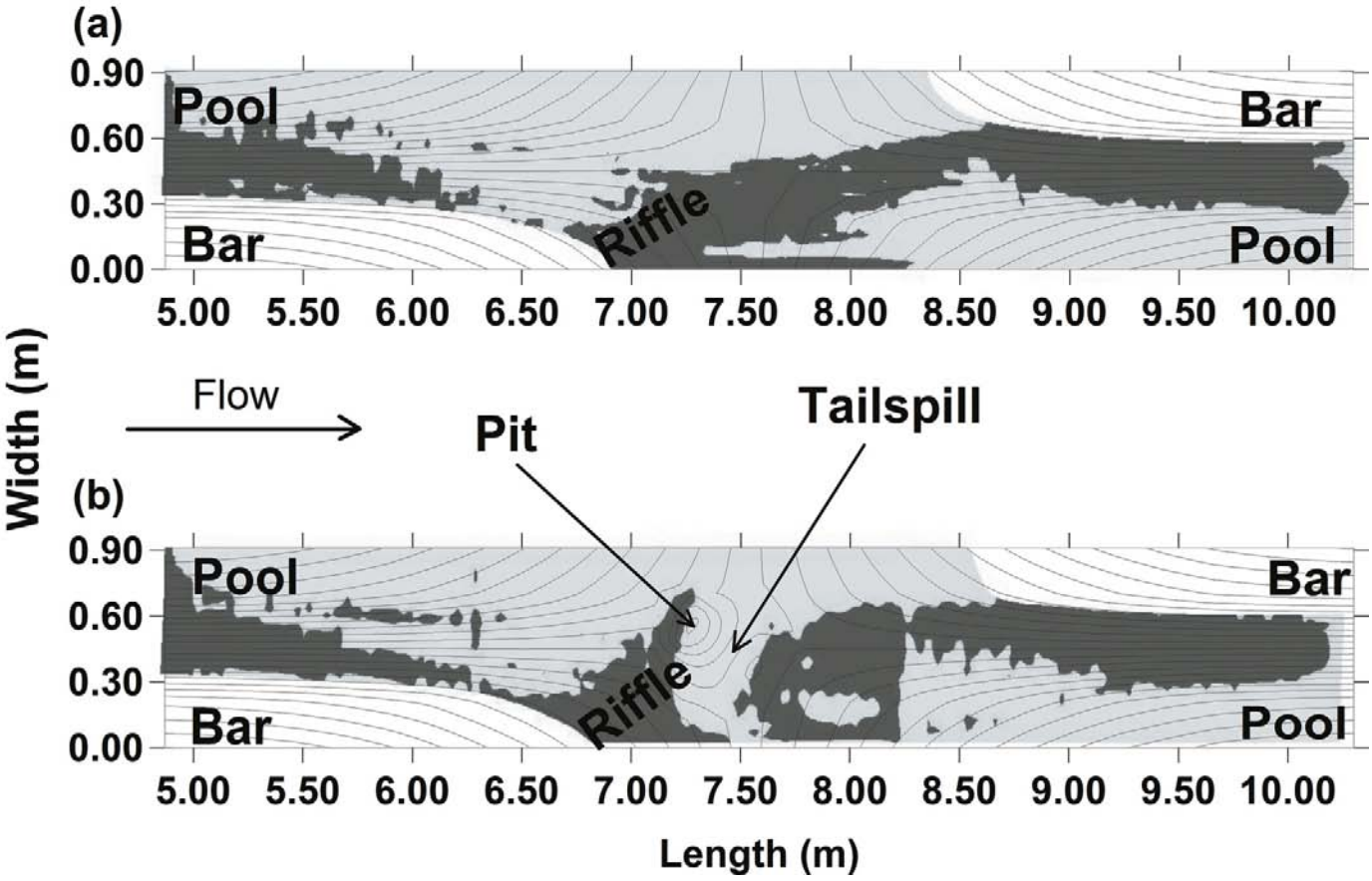

creasing the downwelling flux and reducing reach-average residence times (Fig. 11). Consequently, postspawning hyporheic fluxes are predicted to be larger and more rapid (shorter residence times) than prior to spawning activity.

Model predictions also indicate that the depth of alluvium has little influence on the reach-average downwelling flux and residence time, causing only a slight elongation of the residence time distribution for deeper alluvium (Fig. 11). These results indicate that the bulk of the hyporheic exchange is a near-surface phenomenon in this type of channel, as demonstrated in recent laboratory experiments (Tonina and Buffington 2007).

Oxygen distribution

Predictions indicate that DO concentrations are low within the pool tail prior to spawning, despite downwelling hyporheic flow forced by channel topography (Fig. 12*a*, critical concentration is 5–6 mg·L^{-1}, which equals 50%–60% of saturation for this study). DO concentrations drop to around 30% of saturation in the zone where the middle of the egg pocket would be located and below 20% of saturation at the bottom of where the pocket would be placed. However, once the redd topography is superimposed over the bedform, predicted DO concentrations within the redd increase to 90% and 75% of saturation at the center and bottom of the egg pocket, respectively (Fig. 12*b*). When the combined effects of spawning-related changes in bed topography and hydraulic conductivity are considered, predicted DO concentrations within the egg pocket are comparable with that of the in-stream water (Fig. 12*c*). The change in DO concentration among the three cases shows the importance of the interaction between bed topography, redd topography, and spawning-related changes in hydraulic conductivity.

Discussion

Our analysis confirms that redds induce hyporheic exchange and that a double circulation cell occurs, as observed in laboratory studies of redds (Carling et al. 2006) and two-dimensional dune-like bedforms (Cooper 1965). Furthermore, the three-dimensional nature of our approach shows the spatial complexity, extent, and magnitude of hyporheic flow within a redd located in a typical setting (pool tail) and further quantifies the potential biological significance of redd-induced hyporheic exchange. In particular, the model predicts that the redd creates suitable DO levels and incubation habitat within the egg pocket that otherwise would not occur. Without the redd, only marginally suitable DO levels are predicted in locations where egg pockets would be located, despite the downwelling flow caused by pool–riffle topography. Redd construction at the pool tail significantly enhances the hyporheic velocity and oxygen concentration developed by the pool–riffle topography, increasing the potential for embryo survival. Our three-dimen-

Fig. 8. Predicted hyporheic flow paths along the longitudinal axis of the redd with velocity vectors colored by magnitude. Scales of hyporheic circulation due to the redd versus that of the surrounding pool–riffle topography are indicated. Hydraulic conductivity within the redd (K_{redd}) is 0.05 m·s^{-1} and that of the surrounding sediment (K_{aq}) is 10^{-3} m·s^{-1}. All dimensions are model-scaled.

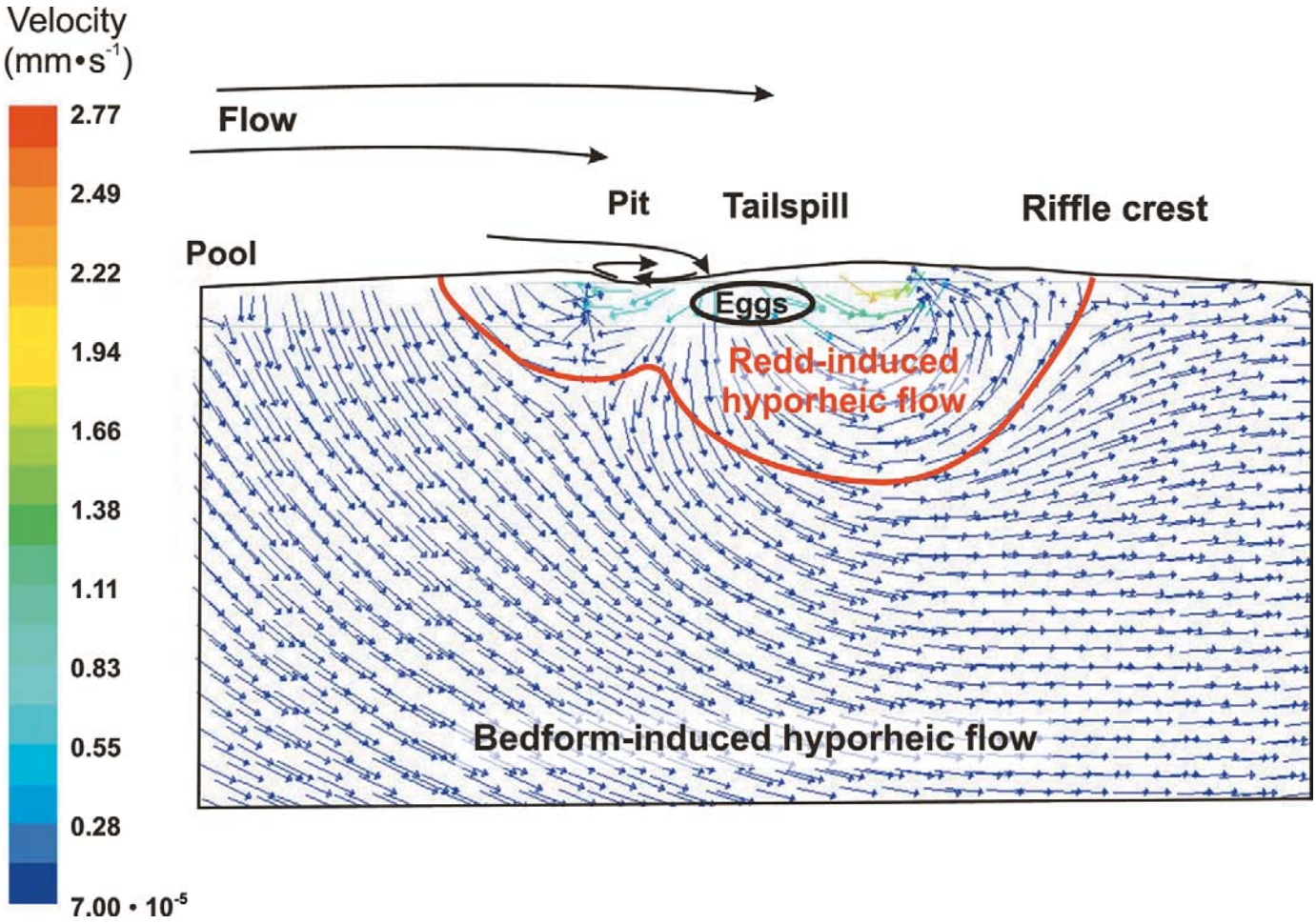

sional model also demonstrates the importance of quantifying local variations in streambed pressure to understand hyporheic flow through redds. The model indicates that local streambed pressure variations about the redd control hyporheic flow through the egg pocket, with redd-induced hyporheic velocities faster than those due solely to the pool–riffle morphology. Previous numerical models examining the effects of redds have not accounted for the influence of redd topography on local streambed pressure and consequent hyporheic flow. For example, the three to fourfold increase of hyporheic velocity resulting from redd topography in our study would not be accounted for with the Alonso et al. (1988) model. Their predicted values of intragravel velocity depended only on modeled variations of hydraulic conductivity and pool–riffle scale changes in streambed pressure. Furthermore, if the spatial variability of upwelling and downwelling around redds is not recognized, local measurements, such as vertical hydraulic gradients (Geist 2000), may yield misleading results. Consequently, we recommend a higher sampling density for those approaches to better represent both the mean and the variance of hyporheic flow through the redd.

The model also predicts that the effects of the redd are localized and nested within, but not superseded by, the hydraulics of the surrounding bedform topography. Furthermore, despite its local influence, the redd has a significant impact on the channel; the presence of one redd is predicted to alter the average hyporheic exchange through the reach. Mass spawning and the occurrence of multiple redds could more strongly influence the reach-average exchange, since the near-bed pressure profile would be more variable and a larger area of the streambed would have higher permeability because of widespread spawning activity. This may lead to shallower, but more intense hyporheic flows, as most of the exchange will be confined to the more permeable portions of the bed disturbed by spawning.

The depth of alluvium can also influence hyporheic path lengths and therefore intragravel velocities (Tonina 2005). However, from our results, we suggest that shallow, short flow paths, such as those related to salmonid redds, are less affected by alluvial depth than deep, long flow paths. Hence, alluvial depth may not have a strong impact on redd-induced hyporheic velocities, except where alluvial depths are comparable with typical redd excavation depths.

The amount of river water pumped into the streambed and the time that it spends traversing the subsurface sediment before reemerging into the stream (residence time) also have important biological implications. Because biological

Fig. 9. Predicted hyporheic pathlines (colored by individual trajectories) for the study reach with (*a*) deep alluvium (0.5λ) and (*b*) shallow alluvium (0.05λ). Insets show the plan view of the upwelling (red) and downwelling (yellow) areas.

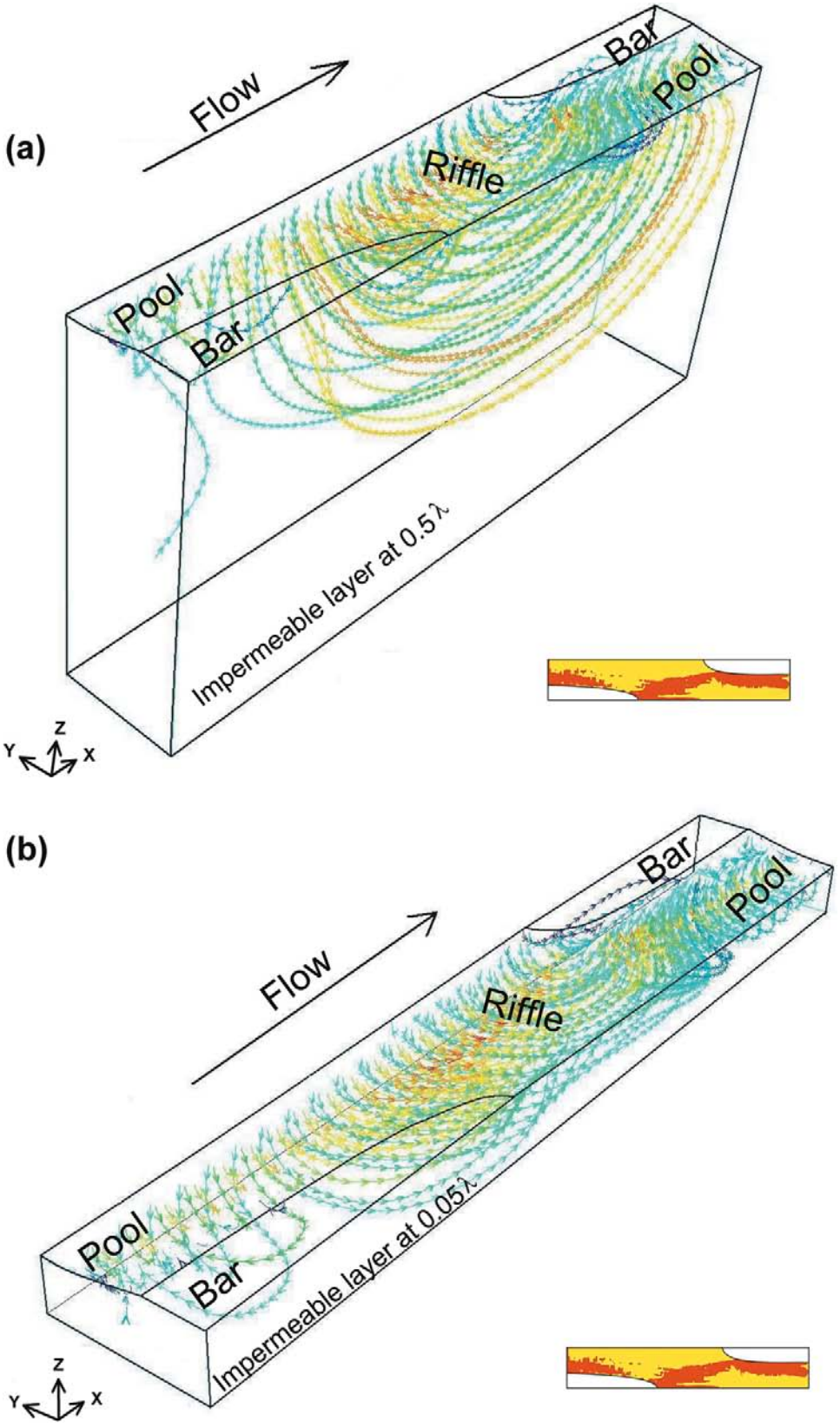

Fig. 10. Vertical profiles of predicted hyporheic velocities at three locations along the longitudinal axis of the redd (below the pit (P1) (squares), below the middle of the tailspill (P2) (circles), and below the tailspill crest (P3) (triangles) for (*a*) deep alluvium (0.5λ) and (*b*) shallow alluvium (0.05λ). Locations of each profile are shown in Fig. 3. Open, solid, and crossed symbols indicate three cases: (1) without redd topography, (2) with redd topography but no spawning-related winnowing of sediment ($K_{redd} = K_{aq} = 10^{-3}$ m·s^{-1} throughout), and (3) with redd topography and spawning-related winnowing ($K_{redd} = 0.05$ m·s^{-1} and $K_{aq} = 10^{-3}$ m·s^{-1} in the surrounding streambed). All plotted values are model-scaled and depth is relative to the original bed surface, with –0.02 and –0.09 m indicating the top and bottom of the egg pocket, respectively.

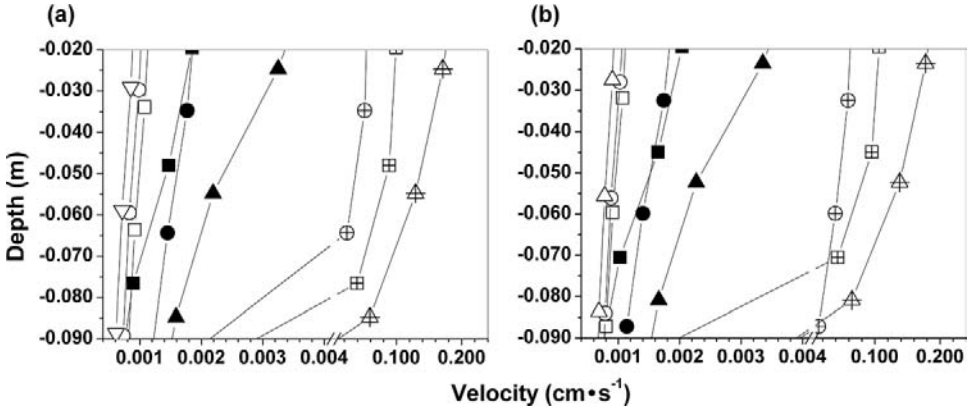

Fig. 11. Predicted reach-average magnitude of downwelling flux as a function of time for (*a*) deep alluvium (0.5λ) and (*b*) shallow alluvium (0.05λ) for three cases: (1) without redd topography, (2) with redd topography but no spawning-related winnowing of sediment ($K_{redd} = K_{aq} = 10^{-3}$ m·s^{-1} throughout), and (3) with redd topography and spawning-related winnowing ($K_{redd} = 0.05$ m·s^{-1} and $K_{aq} = 10^{-3}$ m·s^{-1} in the surrounding streambed). Reported values are downwelling fluxes at 0%, 10%, 25%, 50%, 75%, and 90% of the residence time distribution. The reported hydraulic conductivities are model-scaled.

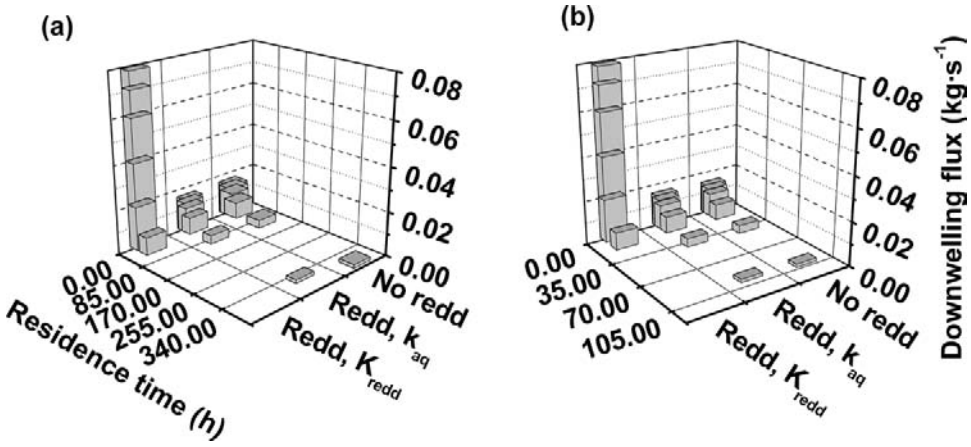

uptake and chemical transformations, such as nitrification and denitrification, require a certain amount of time to take place, residence times must match or exceed reaction times for completion of biochemical processes. Our results show that redds can alter the distribution, intensity, and direction of hyporheic flux, thereby potentially influencing chemical and biological reactions and the fate of in-stream solutes and nutrients, particularly in streams where mass spawning occurs.

Comparison of our results with available field and laboratory measurements is difficult because the subsurface flow field and DO transport depend on site-specific values of hydraulic gradient, sediment conductivity, and chemical reactions. Furthermore, prior studies generally do not offer the detailed measurements needed for testing our three-dimensional model. Nevertheless, some general comparisons can be made. In a laboratory study, Carling et al. (2006) measured velocity distributions in an artificial redd composed of a homogeneous gravel mixture and observed a three-dimensional hyporheic flow field similar to ours (cf. Figs. 8 and 10 with Plate 1 in Carling et al. 2006). Additionally, they indirectly estimated intragravel velocities ranging from 4 to 10 mm·s^{-1} within the redd, comparable with values predicted in our simulation (0.28–2.77 mm·s^{-1}). In a field study, Malcolm et al. (2004) found that DO concentrations within redds were similar to in-stream values (92% and 71% of saturation at 150 and 300 mm depth, respectively), which supports our findings that DO concentrations are close to in-stream values in newly built redds. However, DO concentrations depend on local SOD and may vary greatly among sites, despite similar patterns of hyporheic exchange. Overall, these comparisons are encouraging, but further field or laboratory testing of our model is needed before it can be confidently applied to fisheries research and management. Testing of the model will require spatially detailed measurements of hyporheic exchange using sensor arrays distributed

Fig. 12. Dissolved oxygen concentrations (%saturation and mg·L^{-1}) along a longitudinal profile through the pool and riffle for three cases: (*a*) without redd topography (prespawning reference condition), (*b*) with redd topography alone (undisturbed hydraulic conductivity of 10^{-3} m·s^{-1} throughout), and (*c*) with redd topography and spawning-related winnowing (K_{redd} = 0.05 m·s^{-1} and K_{aq} = 10^{-3} m·s^{-1} in the surrounding streambed). Ellipse denotes the typical location for a Chinook salmon egg pocket. The spatial extent of dissoved oxygen concentrations shown in each panel depends on the solution of eq. 4 for each scenario. Vertical scale differs slightly in each panel and reported hydraulic conductivities are model-scaled.

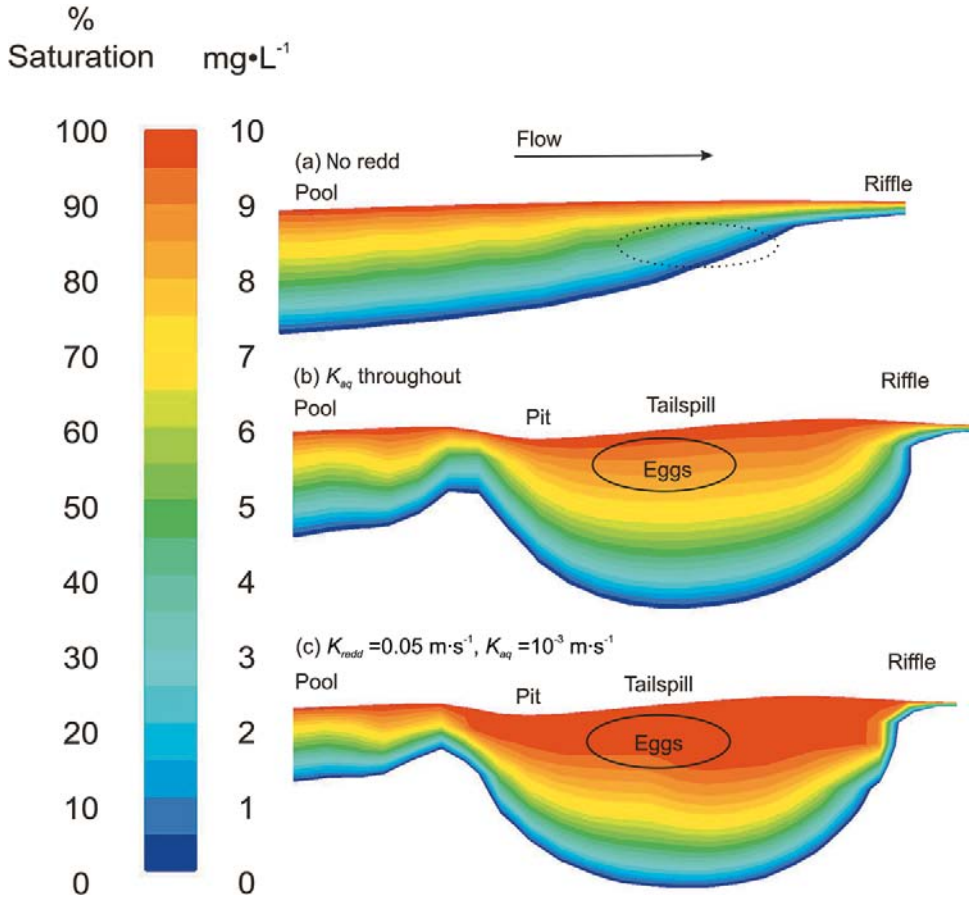

within the streambed, such as temperature probes (Constantz and Thomas 1996), fiber optic cables (Selker et al. 2006), or active carbon granules (Carling et al. 2006).

Results of this study highlight the importance of spawning-related changes in hydraulic conductivity but are based on a simplified treatment of the true spatial variation of sediment characteristics. We focus our analysis on the effects of redd topography and increased hydraulic conductivity relative to the surrounding undisturbed bed material rather than that caused by sediment heterogeneity within the redd. Redds are typically characterized by coarse lag sediments at the base of the egg pocket and a progressive fining toward the surface of the redd (see review by Chapman 1988). Spatial variation in sediment characteristics can generate and intensify hyporheic exchange (Vaux 1962; Salehin et al. 2004), particularly at the base of the egg pocket where the coarse lag rocks are located and around which the eggs are deposited. Hyporheic velocities and rates of solute exchange will likely be greater in the immediate vicinity of the eggs due to the increased hydraulic conductivity of the coarser sediment. In addition, the surrounding streambed may show spatial heterogeneity of grain size (textural patches) due to spatial and temporal variation in streamflow, sediment transport, and erosion/deposition (Buffington and Montgomery 1999; Dietrich et al. 2006), which will likely enhance and modify hyporheic exchange (Sophocleous 1991; Cardenas et al. 2004; Salehin et al. 2004) compared with that predicted for homogeneous sediments. Because we use a fully three-dimensional model, these complexities could be incorporated and explored in future analyses.

Results may also be influenced by postspawning infiltration of fine material that reduces hydraulic conductivity of the redd (e.g., Lapointe et al. 2004) and by postspawning floods that erode and alter the shape of redds, reducing their ability to generate hyporheic exchange. However, these modulating effects tend to be site specific, with some environments showing long-term persistence of both redd topography (DeVries 1997) and spawning-related coarsening of sediment (Gottesfeld et al. 2004), while spawning effects are ephemeral in other locations (Stuart 1953; Everest et al. 1987). Hence, the biological significance of redd-induced hyporheic exchange should be evaluated within the context of the site-specific potential for postspawning floods and fine-sediment infiltration. Although our analysis examines initial conditions immediately after spawning, the dynamic responses discussed above could be evaluated by coupling

our approach with three-dimensional models for bed load transport (to examine fluvial modification of redd topography) and for fine-sediment infiltration within the redd (e.g., Tonina et al. 2008*a*). A potentially important factor to examine in such modeling is whether the sediment stratification created by the female fish during redd construction, with sediment coarsening from top to bottom of the redd, functions as a filter to keep fine sediments from infiltrating deep into the redd and reaching the eggs.

Overall, our findings indicate that salmonid spawning activities likely have a positive influence on survival of their offspring. However, the same activities that enhance embryo survival may make the eggs vulnerable to pollutants and fine sediment that are present in the stream; redd-induced hyporheic flow will direct pollutants and fine sediment into egg pockets that are easily penetrated because of their coarse, open structure and high hydraulic conductivity. However, because the redd sediment is graded from coarse to fine as one moves from the ova to the surface, it may filter and reduce the penetration of fine material and pollutants into the redd.

Although we focus on Chinook salmon, spawning activities and the effects of redds are similar among species (similar redd shape and winnowing effects), with dimensions scaled by fish size. Smaller fish build smaller redds with shallower egg pockets (e.g., Burner 1951). In turn, redd-induced hyporheic flows are less deep, but because the eggs lay closer to the surface, they likely benefit from the same sort of redd-induced hyporheic flows presented here. Consequently, the results of this study are likely applicable to salmonids in general.

Finally, it is worth noting that the model can be generalized to investigate hyporheic exchange and spawning success for different redd sizes and stream environments. Because of its flexibility, the model could be used to generate biological hypotheses that are subsequently tested through field or laboratory studies. For example, an important issue is the relationship among redd dimensions, hyporheic exchange, and spawning success: given that salmon create a distribution of redd sizes within and between species (Burner 1951), are some redd geometries more successful than others? Although, our analysis suggests that higher-amplitude redds will have a stronger hyporheic flow and larger DO values, the model could be used to investigate whether there are critical redd dimensions for successful survival to emergence, similar to thresholds that have been developed for the effects of fine sediment on embryo survival (e.g., Bjornn and Reiser 1991).

Additionally, the effects of redd dimensions on hyporheic flow and spawning success may depend on stream context (e.g., stream size, flow regime, temperature variations, sediment composition, and surrounding bed forms). Stream context may drive selection of redd dimensions that provide the most favorable conditions for embryo development. For example, plane-bed channels, which are expected to have little hyporheic exchange due to a lack of fluvial bedforms (Buffington and Tonina 2009), might select for higher-amplitude redds than in pool–riffle channels, where fish may capitalize on existing hyporheic exchange generated by pool–riffle topography. Similarly, stream size and associated depths of fluvial scour may have a selective effect on the size of spawning fish and associated redd dimensions and egg burial depths (e.g., Montgomery et al. 1999; Tonina et al. 2008*b*). By applying our model in different geomorphic settings, one could explore the potential effects of stream context on redd-induced hyporheic exchange and further develop hypotheses regarding environmental selection of redd dimensions and fish size.

Furthermore, the rate of fluvial alteration of redds may affect embryo survival. As embryos develop, their oxygen requirements increase, whereas hyporheic exchange may decrease due to fluvial erosion of redd topography and reduced hydraulic conductivity from fine-sediment infiltration. The relative rates of these competing effects (fluvial alteration versus embryo growth) may influence survival to emergence, suggesting the existence of a critical rate of fluvial alteration of redds beyond which survival declines. Alternatively, the fluvial environment may drive different life histories, with faster rates of embryo maturity in channels that rapidly modify redd topography and hydraulic conductivity. As discussed above, these dynamic responses could be investigated by coupling our model with three-dimensional sediment transport and infiltration models.

Therefore, not only does the model show that embryo habitat is enhanced by redd construction, but it is also a potential tool for investigating new questions, such as those discussed above.

Acknowledgements

This work was supported by the US Department of Education Fund for the Improvement of Postsecondary Education (P116Z010107) and by the US Forest Service Rocky Mountain Research Station (03-JV-11222014-060). We thank Bruce Rieman for thoughtful comments on an earlier draft of this manuscript, Russ Thurow for his advice on redd characteristics, and Nick Scheidt for field assistance. Additionally, we thank four anonymous reviewers and the assistant editor for comments that improved the paper.

References

Alonso, C.V., Theurer, F.D., and Zachmann, D.W. 1988. Tucannon River offsite study: sediment intrusion and dissolved-oxygen transport model. U.S. Department of Agriculture, Agricultural Research Service, Hydro-Ecosystems Research Group, Fort Collins, Co.

Andrews, E.D. 1984. Bed-material entrainment and hydraulic geometry of gravel-bed rivers in Colorado. Geol. Soc. Am. Bull. **95**(3): 371–378. doi:10.1130/0016-7606(1984)95<371:BEAHGO>2.0.CO;2.

Baxter, C.V., and Hauer, R.F. 2000. Geomorphology, hyporheic exchange, and selection of spawning habitat by bull trout (*Salvelinus confluentus*). Can. J. Fish. Aquat. Sci. **57**(7): 1470–1481. doi:10.1139/cjfas-57-7-1470.

Bjornn, T.C., and Reiser, D.W. 1991. Habitat requirements of salmonids in streams. *In* Influence of forest and rangeland management on salmonid fishes and their habitats. *Edited by* W.R. Meehan. Am. Fish. Soc. Spec. Publ. 19. American Fisheries Society, Bethesda, Md. pp. 83–138.

Buffington, J.M., and Montgomery, D.R. 1999. Effects of hydraulic roughness on surface textures of gravel-bed rivers. Water Resour. Res. **35**(11): 3507–3521. doi:10.1029/1999WR900138.

Buffington, J.M., and Tonina, D. 2009. Hyporheic exchange in mountain rivers II: Effects of channel morphology on me-

chanics, scales and rates of exchange. Geogr. Compass, **3**(3): 1038–1062. doi:10.1111/j.1749-8198.2009.00225.x.

Burner, C.J. 1951. Characteristics of spawning nests of Columbia River salmon. Fish. Bull. (Washington, D.C.), **52**: 97–110.

Cardenas, M.B., Wilson, J.L., and Zlotnik, V.A. 2004. Impact of heterogeneity, bed forms, and stream curvature on subchannel hyporheic exchange. Water Resour. Res. **40**(8): W08307. doi:10.1029/2004WR003008.

Carling, P.A., and Orr, H.G. 2000. Morphology of riffle–pool sequences in the River Severn, England. Earth Surf. Process. Landf. **25**(4): 369–384. doi:10.1002/(SICI)1096-9837(200004)25:4<369::AID-ESP60>3.0.CO;2-M.

Carling, P.A., Whitcombe, L.J., Benson, I.A., Hankin, B.G., and Radecki-Pawlik, A.M. 2006. A new method to determine interstitial flow patterns in flume studies of sub-aqueous gravel bedforms such as fish nests. River Res. Appl. **22**(6): 691–701. doi:10.1002/rra.930.

Chadwick, A., and Morfett, J. 1997. Hydraulics in civil and environmental engineering. E & FN Spon, London, U.K.

Chapman, D.W. 1988. Critical review of variables used to define effects of fines in redds of large salmonids. Trans. Am. Fish. Soc. **117**(1): 1–21. doi:10.1577/1548-8659(1988)117<0001:CROVUT>2.3.CO;2.

Chapman, W.M. 1943. The spawning of chinook salmon in the main Columbia River. Copeia, **3**: 1968–1970.

Coble, D.W. 1961. Influence of water exchange and dissolved oxygen in redds on survival of steelhead trout embryos. Trans. Am. Fish. Soc. **90**(4): 469–474. doi:10.1577/1548-8659(1961)90[469:IOWEAD]2.0.CO;2.

Constantz, J., and Thomas, C.L. 1996. The use of streambed temperature profiles to estime the depth, duration, and rate of percolation beneath arroyos. Water Resour. Res. **32**(12): 3597–3602. doi:10.1029/96WR03014.

Cooper, A.C. 1965. The effect of transported stream sediments on the survival of sockeye and pink salmon eggs and alevin. Int. Pac. Salmon Fish. Comm. Bull. 18. International Pacific Salmon Fisheries Commission, New Westminster, B.C.

Darcy, H. 1856. Les fontaines publiques de la ville de Dijon. Libraire des Corps Imperiaux des Ponts et Chaussées et des Mines, Dalmont, Paris, France.

DeVries, P. 1997. Riverine salmonid egg burial depths: a review of published data and implications for scour studies. Can. J. Fish. Aquat. Sci. **54**(8): 1685–1698. doi:10.1139/cjfas-54-8-1685.

Dietrich, W.E., and Smith, D.J. 1983. Influence of the point bar on flow through curved channels. Water Resour. Res. **19**(5): 1173–1192. doi:10.1029/WR019i005p01173.

Dietrich, W.E., Nelson, P.A., Yager, E., Venditti, J.G., Lamb, M.P., and Collins, L. 2006. Sediment patches, sediment supply and channel morphology. *In* Proceedings of the 4th Conference on River, Coastal and Estuarine: Morphodynamics, 4–7 October 2005, Urbana, Ill.. A.A. Balkema, Rotterdam, The Netherlands. pp. 79–90.

Edwards, R.T. 1998. The hyporheic zone. *In* River ecology and management: Lessons from the Pacific coastal ecoregion. *Edited by* R.J. Naiman and R.E. Bilby. Springer-Verlag, New York. pp. 399–429.

Everest, F.H., Beschta, R.L., Scrivener, J.C., Koski, K.V., Sedell, J.R., and Cederholm, J.C. 1987. Fine sediment and salmonid production: a paradox. *In* Streamside management: forestry and fishery interactions. *Edited by* E.O. Salo and T.W. Cundy. Institute of Forest Resources, University of Washington, Seattle, Wash. pp. 98–142.

Findlay, S., and Sobczak, W.V. 1999. Microbial communities in hyporheic sediments. *In* Streams and ground waters. *Edited by* J.B. Jones and P.J. Mulholland. Academic Press, San Diego, Calif. pp. 287–306.

Fluent Inc. 2003. Fluent user's guide. Distributor: Fluent US, Lebanon, N.H.

Freeze, R.A., and Cherry, J.A. 1979. Groundwater. Prentice Hall, Englewood Cliffs, N.J.

Geist, D.R. 2000. Hyporheic discharge of river water into fall chinook salmon (*Oncorhynchus tshawytscha*) spawning areas in the Hanford Reach, Columbia River. Can. J. Fish. Aquat. Sci. **57**(8): 1647–1656. doi:10.1139/cjfas-57-8-1647.

Geist, D.R. 2005. Conceptual spawning habitat model to aid in ESA recovery plans for Snake River fall Chinook salmon. 2002–2003 Annual Report. Project No. 1199406900 BPA Report DOE/BP-00000652-21. Bonneville Power Administration, Portland, Ore.

Geist, D.R., and Dauble, D.D. 1998. Redd site selection and spawning habitat use by fall Chinook salmon: the importance of geomorphic features in large rivers. Environ. Manag. **22**(5): 655–669. doi:10.1007/s002679900137. PMID:9680535.

Gottesfeld, A.S., Hassan, M.A., Tunnicliffe, J.F., and Poirier, R.W. 2004. Sediment dispersion in salmon spawning streams: the influence of floods and salmon redd construction. J. Am. Water Resour. Assoc. **40**(4): 1071–1086. doi:10.1111/j.1752-1688.2004.tb01068.x.

Greig, S.M., Sear, D.A., and Carling, P.A. 2005. The impact of fine sediment accumulation on the survival of incubating salmon progeny: implications for sediment management. Sci. Total Environ. **344**(1-3): 241–258. doi:10.1016/j.scitotenv.2005.02.010. PMID:15893806.

Greig, S.M., Sear, D.A., and Carling, P.A. 2007. A review of factors influencing the availability of dissolved oxygen to incubating salmonid embryos. Hydrol. Process. **21**(3): 323–334. doi:10.1002/hyp.6188.

Groot, C., and Margolis, L. 1991. Pacific salmon life histories. Columbia Press, Vancouver, B.C.

Gustafson-Greenwood, K.I., and Moring, J.R. 1991. Gravel compaction and permeabilities in redds of Atlantic salmon, *Salmo salar* L. Aquacult. Fish. Manag. **22**(4): 537–540.

Hanrahan, T.P. 2007. Bedform morphology of salmon spawning areas in a large gravel-bed river. Geomorphology, **86**(3-4): 529–536. doi:10.1016/j.geomorph.2006.09.017.

Hendricks, S.P., and White, D.S. 1991. Physico-chemical patterns within a hyporheic zone of a northern Michigan river, with comments on surface water patterns. Can. J. Fish. Aquat. Sci. **48**(9): 1645–1654. doi:10.1139/f91-195.

Hirt, C.W., and Nichols, B.D. 1981. Volume of fluid (VOF) method for the dynamics of free boundaries. J. Comput. Phys. **39**(1): 201–225. doi:10.1016/0021-9991(81)90145-5.

Hodskinson, A. 1996. Computational fluid dynamics as a tool for investigating separated flow in river bends. Earth Surf. Process. Landf. **21**(11): 993–1000. doi:10.1002/(SICI)1096-9837(199611)21:11<993::AID-ESP698>3.0.CO;2-R.

Huang, G., Tamai, N., and Ishida, H. 2001. Characterization of dissolved oxygen depletion in Lake Yanaka. *In* Proceedings of the 29th Congress of the International Association of Hydraulic Engineering and Research, 16–21 September 2001, Beijing, China. International Association of Hydraulic Engineering and Research, Madrid, Spain. pp. 747–752.

Keller, E.A., and Melhorn, W.N. 1978. Rhythmic spacing and origin of pools and riffles. Geol. Soc. Am. Bull. **89**(5): 723–730. doi:10.1130/0016-7606(1978)89<723:RSAOOP>2.0.CO;2.

King, J., and Thurow, R. 2000. Completion report sediment monitoring techniques validation. USDA Forest Service, Rocky Mountain Research Station, Boise, Idaho.

Kondolf, M.G. 2000. Assessing salmonid spawning gravel quality. Trans. Am. Fish. Soc. **129**(1): 262–281. doi:10.1577/1548-8659(2000)129<0262:ASSGQ>2.0.CO;2.

Lapointe, M.F., Bergeron, N., Bérubé, F., Pouliot, M.-A., and Johnston, P. 2004. Interactive effects of substrate sand and silt contents, redd-scale hydraulic gradients, and interstitial velocities on egg-to-emergence survival of Atlantic salmon (*Salmo salar*). Can. J. Fish. Aquat. Sci. **61**(12): 2271–2277. doi:10.1139/f04-236.

Leopold, L.B., Wolman, M.G., and Miller, J.P. 1964. Fluvial processes in geomorphology. W.H. Freeman, San Francisco, Calif.

Lisle, T.E., and Hilton, S. 1992. The volume of fine sediment in pools: an index of sediment supply in gravel-bed streams. Water Resour. Bull. **28**(2): 371–382.

Ma, L., Ashworth, P.J., Best, J.L., Elliott, L., Ingham, D.B., and Whitcombe, L.J. 2002. Computational fluid dynamics and the physical modelling of an upland urban river. Geomorphology, **44**(3-4): 375–391. doi:10.1016/S0169-555X(01)00184-2.

Malcolm, I.A., Soulsby, C., Youngson, A.F., Hannah, D.M., McLaren, I.S., and Thorne, A. 2004. Hydrological influences on hyporheic water quality: implications for salmon egg survival. Hydrol. Process. **18**(9): 1543–1560. doi:10.1002/hyp.1405.

McLean, S.R., and Smith, D.J. 1986. A model for flow over a two-dimensional bed form. J. Hydraul. Eng. **112**(4): 300–317. doi:10.1061/(ASCE)0733-9429(1986)112:4(300).

McNeil, W.J., and Ahnell, W.H. 1964. Success of pink salmon spawning relative to size of spawning bed materials. Spec. Sci. Rep. Fish. No. 469. US Fish and Wildlife Service, Washington, D.C.

Middleton, G.V., and Southard, J.B. 1984. Mechanics of sediment movement. Short course 3. Society for Economic Paleontologists and Mineralogists, Tulsa, Okla.

Montgomery, D.R., Buffington, J.M., Peterson, N.P., Schuett-Hames, D., and Quinn, T.P. 1996. Stream-bed scour, egg burial depths, and the influence of salmonid spawning on bed surface mobility and embryo survival. Can. J. Fish. Aquat. Sci. **53**(5): 1061–1070. doi:10.1139/cjfas-53-5-1061.

Montgomery, D.R., Beamer, E.M., Pess, G.R., and Quinn, T.P. 1999. Channel type and salmonid spawning distribution and abundance. Can. J. Fish. Aquat. Sci. **56**(3): 377–387. doi:10.1139/cjfas-56-3-377.

Nicholas, A.P., and Sambrook Smith, G.H. 1999. Numerical simulation of three-dimensional flow hydraulic in a braided channel. Hydrol. Process. **13**(6): 913–929. doi:10.1002/(SICI)1099-1085(19990430)13:6<913::AID-HYP764>3.0.CO;2-N.

Packman, A.I., and Bencala, K.E. 1999. Modeling methods in study of surface–subsurface hydrological interactions. *In* Streams and ground waters. *Edited by* J.B. Jones and P.J. Mulholland. Academic Press, San Diego, Calif. pp. 45–80.

Packman, A.I., Salehin, M., and Zaramella, M. 2004. Hyporheic exchange with gravel beds: basic hydrodynamic interactions and bedform-induced advective flows. J. Hydraul. Eng. **130**(7): 647–656. doi:10.1061/(ASCE)0733-9429(2004)130:7(647).

Parker, G. 1978. Self-formed straight rivers with equilibrium banks and mobile bed. Part 2. The gravel river. J. Fluid Mech. **89**(1): 127–146. doi:10.1017/S0022112078002505.

Prestegaard, K.L. 1983. Bar resistance in gravel bed steams at bankfull stage. Water Resour. Res. **19**(2): 472–476. doi:10.1029/WR019i002p00472.

Quinn, T.P. 2005. The behavior and ecology of Pacific salmon and trout. University of Washington Press, Seattle, Wash.

Raudkivi, A.J. 1963. Study of sediment ripple formation. J. Hydraul. Div. (ASCE), **89**(HY6): 15–33.

Ruff, J.F., and Gelhar, L.W. 1972. Turbulent shear flow in porous boundary. J. Eng. Mech. Div. (ASCE), **98**(EM4).

Salehin, M., Packman, A.I., and Paradis, M. 2004. Hyporheic exchange with heterogeneous streambeds: laboratory experiments and modeling. Water Resour. Res. **40**(11): W11504. doi:10.1029/2003WR002567.

Schuett-Hames, D.E. 1996. Effects of scour and fill on salmonid incubation habitat in Kennedy Creek, a low-gradient alluvial channel in Mason and Thurston counties, Washington. M.S. thesis, The Evergreen State College, Olympia, Wash.

Selker, J.S., Thévenaz, L., Huwald, H., Mallet, A., Luxemburg, W., van de Giesen, N., Stejskal, M., Zeman, J., Westhoff, M., and Parlange, M.B. 2006. Distributed fiber-optic temperature sensing for hydrologic systems. Water Resour. Res. **42**(12): W12202. doi:10.1029/2006WR005326.

Shih, T.H., Liou, W.W., Shabbir, A., Yang, Z., and Zhu, J. 1995. A new κ–ε eddy-viscosity model for high Reynolds number turbulent flows — model development and validation. Comput. Fluids, **24**(3): 227–238. doi:10.1016/0045-7930(94)00032-T.

Sophocleous, M.A. 1991. Stream-floodwave propagation through the Great Bend alluvial aquifer, Kansas: field measurements and numerical simulations. J. Hydrol. (Amst.), **124**(3-4): 207–228. doi:10.1016/0022-1694(91)90015-A.

Stuart, T.A. 1953. Spawning migration, reproduction and young stage of loch trout (*Salmo trutta* L.). Rep. No. 5. Freshwater and Salmon Fisheries Research, Scotland.

Stuart, T.A. 1956. The selection of spawning sites by trout. Proc. Linn. Soc. Lond. **167**: 74–76.

Thibodeaux, L.J., and Boyle, J.D. 1987. Bedform-generated convective transport in bottom sediment. Nature, **325**: 341–343. doi:10.1038/325341a0.

Tonina, D. 2005. Interaction between river morphology and intragravel flow paths within the hyporheic zone. Ph.D. dissertation, University of Idaho, Boise, Idaho.

Tonina, D., and Buffington, J.M. 2007. Hyporheic exchange in gravel-bed rivers with pool–riffle morphology: laboratory experiments and three-dimensional modeling. Water Resour. Res. **43**(1): W01421. doi:10.1029/2005WR004328.

Tonina, D., and Buffington, J.M. 2009. Hyporheic exchange in mountain rivers I: Mechanics and environmental effects. Geogr. Compass, **3**(3): 1063–1086. doi:10.1111/j.1749-8198.2009.00226.x.

Tonina, D., Bellin, A., and Marzadri, A. 2008*a*. Modeling fine sediment infiltration within the hyporheic zone. Eos Trans. AGU, **89**(53). [Abstract H11B-0758.]

Tonina, D., Luce, C.H., Rieman, B., Buffington, J.M., Goodwin, P., Clayton, S.R., Ali, S.M., Barry, J.J., and Berenbrock, C. 2008*b*. Hydrological responses to timber harvest in northern Idaho: implications for channel scour and persistence of salmonids. Hydrol. Process. **22**(17): 3223–3235. doi:10.1002/hyp.6918.

Tóth, J. 1963. A theoretical analysis of groundwater flow in small drainage basins. J. Geophys. Res. **68**(16): 4795–4812.

Vaux, W.G. 1962. Interchange of stream and intragravel water in a salmon spawning riffle. Spec. Sci. Rep. Fish. No. 405. US Fish and Wildlife Service, Bureau of Commercial Fisheries, Washington, D.C.

Vollmer, S., de los Santos Ramos, F., Daebel, H., and Kühn, G. 2002. Micro scale exchange processes between surface and subsurface water. J. Hydrol. (Amst.), **269**(1-2): 3–10. doi:10.1016/S0022-1694(02)00190-7.

Vronskiy, B.B. 1972. Reproductive biology of the Kamchatka River chinook salmon (*Oncorhynchus tshawytscha* (Walbaum)). J. Ichthyol. **12**: 259–273.

Wetzel, R.G. 1983. Limnology. 2nd ed. Hart Brace Jovanovich College Publishers, New York.

White, D.S. 1990. Biological relationships to convective flow pat-

terns within stream beds. Hydrobiologia, **196**(2): 149–158. doi:10.1007/BF00006106.

Whiting, P.J., Stamm, J.F., Moog, D.B., and Orndorff, R.L. 1999. Sediment-transporting flows in headwater streams. Geol. Soc. Am. Bull. **111**(3): 450–466. doi:10.1130/0016-7606(1999)111<0450:STFIHS>2.3.CO;2.

Wilke, C.R., and Chang, P. 1955. Correlation of diffusion coefficients in dilute solutions. Am. Inst. Chem. Eng. J. **1**(2): 264–270. doi:10.1002/aic.690010222.

Zimmermann, A.E., and Lapointe, M.F. 2005*a*. Intergranular flow velocity through salmonid redds: sensitivity to fines infiltration from low intensity sediment transport events. River Res. Appl. **21**(8): 865–881. doi:10.1002/rra.856.

Zimmermann, A.E., and Lapointe, M.F. 2005*b*. Sediment infiltration traps: their use to monitor salmonid spawning habitat in headwater tributaries of the Cascapédia River, Québec. Hydrol. Process. **19**(20): 4161–4177. doi:10.1002/hyp.5879.